ORIGINAL ARTICLE

New transluminal attenuation gradient derived from dynamic coronary CT angiography: diagnostic ability of ischemia detected by ^{13}N-ammonia PET

Tsukasa Kojima[1,2] · Michinobu Nagao[3] · Hidetake Yabuuchi[4] · Yuzo Yamasaki[5] · Takashi Shirasaka[2] · Masateru Kawakubo[4] · Kenji Fukushima[6] · Toyoyuki Kato[2] · Atsushi Yamamoto[7] · Risako Nakao[7] · Akiko Sakai[7] · Eri Watanabe[7] · Shuji Sakai[3]

Abstract

Coronary computed tomography angiography (CCTA) has low specificity for detecting significant functional coronary stenosis. We developed a new transluminal attenuation gradient (TAG)-derived dynamic CCTA with dose modulation, and we investigated its diagnostic performance for myocardial ischemia depicted by ^{13}N-ammonia positron emission tomography (PET). Data from 48 consecutive patients who had undergone both dynamic CCTA and ^{13}N-ammonia PET were retrospectively analyzed. Dynamic CCTA was continuously performed in mid-diastole for five cardiac cycles with prospective electrocardiography gating after a 10-s contrast medium injection. One scan of the dynamic CCTA was performed as a boost scan for conventional CCTA at the peak phase of the ascending aorta. Absolute TAG values at five phases around the boost scan were calculated. The dynamic TAG index (DTI) was defined as the ratio of the maximum absolute TAG to the standard deviation of five TAG values. We categorized the coronary territories as non-ischemia or ischemia based on the ^{13}N-ammonia PET results. A receiver operating characteristic (ROC) analysis was performed to determine the optimal cutoff of the DTI for identifying ischemia. The DTI was significantly higher for ischemia compared to non-ischemia (8.8 ± 3.9 vs. 4.6 ± 2.0, $p < 0.01$). The ROC analysis revealed 5.60 as the optimal DTI cutoff to detect ischemia, with an area under the curve of 0.87, 85.7% sensitivity, and 76.2% specificity. TAG provided no additional diagnostic value for the detection of ischemia. We propose the DTI derived from dynamic CCTA as a novel coronary flow index. The DTI is a valid technique for detecting functional coronary stenosis.

Keywords Coronary computed tomography angiography · Coronary artery disease · Positron emission tomography · Transluminal attenuation gradient · 320-Row CT

✉ Michinobu Nagao
nagao.michinobu@twmu.ac.jp

1   Department of Health Sciences, Graduate School of Medical Sciences, Kyushu University, Fukuoka, Japan

2   Division of Radiology, Department of Medical Technology, Kyushu University Hospital, Fukuoka, Japan

3   Department of Diagnostic Imaging and Nuclear Medicine, Tokyo Women's Medical University, 8-1 Kawada-cho, Shinjuku-ku, Tokyo 162-8666, Japan

4   Department of Health Sciences, Faculty of Medical Sciences, Kyushu University, Fukuoka, Japan

5   Departments of Clinical Radiology, Graduate School of Medical Sciences, Kyushu University, Fukuoka, Japan

6   Department of Nuclear Medicine, Saitama Medical University, Saitama, Japan

7   Department of Cardiology, Tokyo Women's Medical University, Tokyo, Japan

Introduction

Coronary computed tomography angiography (CCTA) is a well-known, reliable method for detecting coronary stenosis in clinical workups of coronary artery disease (CAD) [1]. However, the anatomic assessment by CCTA using the criterion of diameter stenosis > 50% does not correlate well with the functional assessment of the fractional flow reserve (FFR), which is regarded as the gold standard for determining hemodynamically significant coronary stenosis [2–4]. To overcome the weaknesses of conventional CCTA, the transluminal attenuation gradient (TAG) [5–7], myocardial perfusion CT [8–10], and noninvasive fractional flow reserve-CT (FFR-CT) [11–13] were recently introduced, and their ability to assess physiological consequences during CT examinations has been tested. There has been progress in designing functional evaluations by myocardial perfusion CT and FFR-CT, but myocardial perfusion CT requires additional radiation exposure and contrast agents to scan at the stress and rest conditions [14]. In addition, FFR-CT involves high cost and long analysis times.

In contrast, TAG is calculated using a CCTA image acquired with a single contrast injection, and it is obtained without using special software. TAG is calculated by obtaining the linear regression coefficient between the luminal contrast attenuation and the distance along the vessel from the coronary ostium [5, 7, 15, 16]. The use of TAG can assist in the noninvasive assessment of hemodynamically significant coronary artery stenosis and flow [5–7]. However, several studies have reported that TAG has no incremental diagnostic value for the assessment of the hemodynamic consequences of coronary stenosis [17, 18]. One reason for this is that TAG depends on the scan timing after the injection of the contrast medium (CM) [19]; in that study, Funama et al. observed that the optimal scan time point for TAG is before rather than after the peak enhancement of coronary arteries. In other words, the scan timing of the peak contrast enhancement of coronary arteries is not suitable for obtaining the optimal TAG value.

However, TAG is generally calculated from a CCTA image obtained at the time point of the peak enhancement of coronary arteries. This might lower the diagnostic utility of the TAG. Another index that does not depend on the scan timing is thus required for the detection of ischemia. We hypothesized that the use of multi-phase TAGs around the peak contrast enhancement phase (including the optimal TAG) would improve the diagnostic ability to detect significant coronary artery stenosis.

[13]N-ammonia PET-MPI offers very high sensitivity, specificity, and overall diagnostic accuracy for the detection of myocardial ischemia [20–25]. The clinical superiority of ^{13}N-ammonia PET-MPI was recognized in a joint statement of the American Society of Nuclear Cardiology and Society of Nuclear Medicine and Molecular Imaging [26]. Herein, we propose a new dynamic TAG index (DTI) derived from dynamic 320-row CCTA (dynamic CCTA), and we conducted the present study to determine the diagnostic performance of the DTI for the detection of myocardial ischemia based on the ^{13}N-ammonia PET-MPI results.

Materials and methods

Study population

We retrospectively analyzed the data of 48 consecutive patients who had undergone both dynamic CCTA and rest/adenosine stress ^{13}N-ammonia positron emission tomography myocardial perfusion imaging (PET-MPI). All patients had been clinically referred for the assessment of known or suspected coronary artery disease (CAD). The CCTA was performed first for each patient, and ^{13}N-ammonia PET-MPI was then performed to assess the presence of myocardial ischemia. In all patients, ^{13}N-ammonia PET was performed within 3 months after the CCTA examination. Revascularization therapy was not performed during the interval.

The patient exclusion were as follows: (i) acute myocardial infarction (within 3 months); (ii) unstable angina (recent onset of angina within 1 month, or severe and worsening clinical symptoms); (iii) chronic atrial fibrillation; (iv) pregnancy, hyperthyroidism, or known allergic reaction to contrast media; (v) severe left ventricular dysfunction (left ventricular ejection fraction < 20%); (vi) known history of bronchial asthma; (vii) congestive heart failure (New York Heart Association class IV); and (viii) greater than first-degree atrioventricular block. A detailed medical history was recorded for each patient, with particular attention to evidence of hypertension, diabetes mellitus, and hyperlipidemia. All patients underwent a battery of laboratory tests, including tests for traditional atherosclerotic risk factors. The CAD risk factors considered in this study were hypertension, diabetes mellitus, hyperlipidemia, and smoking history. The patients' characteristics are summarized in Table 1. After the study's protocol was approved by the local ethics committee, informed consent for this retrospective analysis was obtained from all of the patients.

The CCTA scan conditions

All patients were examined on a 320-row CT scanner (Aquilion One Genesis Edition, Canon Medical Systems, Otawara, Japan). First, a test-bolus examination was performed using prospective electrocardiography

Table 1 Characteristics of 48 the patients with CAD

Clinical characteristic	
Male (%)	29 (60%)
Age (years, mean ± SD)	71 ± 9.6
Body mass index (mean ± SD)	22 ± 2.3
Hypertension (%)	29 (60%)
Diabetes mellitus (%)	16 (33%)
Hyperlipidemia (%)	23 (48%)
eGFR (ml/min/1.73 m^2, mean ± SD)	62 ± 9.5
Current smoker (%)	4 (8%)
Past smoker (%)	18 (38%)
Coronary artery calcium score (mean ± SD)	252 ± 608

eGFR estimated glomerular filtration rate
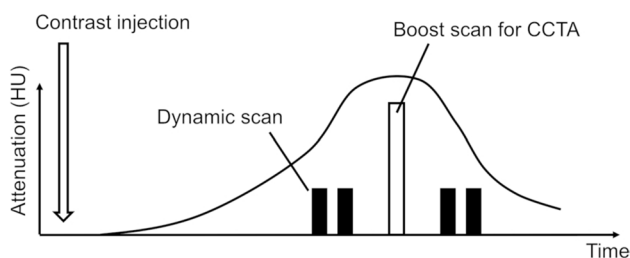
Fig. 1 Overview of the dynamic-CCTA methods

(ECG)-gating axial scans at the ascending aorta at the slice level of the pulmonary trunk in mid-diastole for 15–25 cardiac cycles during a 20.0-s period starting at 7.0 s after the initiation of the bolus injection of the CM to determine the optimal scan timing for 320-row CCTA [27].

After the test-bolus examination, a dynamic CCTA scan was continuously performed in mid-diastole for five cardiac cycles with prospective ECG-gating axial scans after a 10-s CM injection of Iopamidol-370 (370 mgI/ml Iopamiron; Bayer HealthCare, Osaka, Japan) [42 ml (27–53 ml), 259 mgI/kg]. One scan of the dynamic CCTA was performed as a boost scan for standard CCTA at the peak phase of the ascending aorta, which was determined by the test-bolus examination (Fig. 1). The acquisition parameters are summarized in Table 2. The standard CCTA was analyzed using a workstation (Ziosoft, Tokyo, Japan) based on a combination of transverse sections and the automatically generated curved multiplanar reconstruction (MPR) images of the target vessels. A semi-automated vessel analysis tool was used for grading the severity of stenosis. Images were clinically interpreted by the consensus decision of two experienced radiologists, using the American Heart Association (AHA) 15-segment model [28]. Significant stenosis was defined as ≥ 50% stenosis in a major epicardial coronary artery segment with a dia. ≥ 2 mm [29].

Table 2 The dynamic and boost CCTA scan parameters

Parameter	Dynamic scan	Boost scan
Beam collimation (mm)	320 × 0.5	320 × 0.5
Tube voltage (kVp)	100	100
Tube current (mA)	80	700
Rotation time (s)	0.275	0.275
Contrast material dose (mgI/kg)	259	
Injection duration (s)	10	
Iterative reconstruction, AIDR 3D	Standard	Standard
Slice thickness (mm)	0.5	0.5
Slice intervals (mm)	0.25	0.25

AIDR rt3D, adaptive iterative dose reduction 3D

Image analysis with some TAGs for dynamic CCTA

We performed the TAG analysis with a semi-automated method using a dedicated workstation (Vitrea, Canon Medical Systems, Otawara, Japan). The vessel centerline and contouring were automatically determined for each major coronary artery and were manually corrected if necessary. The RCA started at the ostial and ended the #3, LAD started at the ostial left coronary artery and ended the #8, and LCX started at the ostial left coronary artery and ended the #13. Cross-sectional images perpendicular to the vessel centerline were then reconstructed. The mean value of the luminal area was measured in Hounsfield units (HU) at 1-mm intervals, from the ostium to a distal level where the cross-sectional minimal area fell below 2.0 mm^2. The data points in segments with motion or blooming artifacts from luminal calcium were manually excluded from the analysis. TAG is expressed as the change in HU per 10-mm length of coronary artery, defined as the linear regression coefficient between the intraluminal radiological attenuation and the distance from the ostium [5, 7, 15, 16, 30].

Absolute TAG values at five phases around the boost scan were calculated. We defined the DTI as the ratio of the maximum absolute TAG (TAG_{max}) to the standard deviation (SD) of five TAGs (Fig. 2). The TAG of the boost scan was defined as the 'conventional TAG (C-TAG)'. The DTI and the C-TAG were determined for each of the RCA, LAD, and LCX.

Rest/adenosine stress ^{13}N-ammonia PET-MPI

[13]N-ammonia PET images were obtained on a whole-body 64-row PET/CT scanner (Biograph-mCT®, Siemens Healthcare, Erlangen, Germany) with the 3D list mode protocol. A low-dose CT transmission scan was performed with respiratory gating or shallow-expiration breath-holding for attenuation correction. A 10-min 3D list mode scan was performed for both rest and stress within the interval of sufficient radioactive decay (40 min). For both the rest and stress scans, 740 MBq of ^{13}N-ammonia was used from the right basilica vein via an automatic syringe pump, followed by 20 mL of saline at 40 mL/min. Adenosine stress (0.12 mg/min/kg) was administered 3 min prior to the stress scan and continued for 6 min.

Static and electrocardiogram-gated (16 bin) images were resampled from the list-mode data (120–600 s) and exported as a polar map using a 17-segment model. PET images were interpreted by two experienced cardiologists and a nuclear medicine physician. A summed differential score (SDS) > 2 per each coronary territory was defined as positive for myocardial ischemia. The SDS is the difference between the summed rest score (SRS) and summed stress score (SSS), representing the severity of ischemia. Based on each patient's ^{13}N-ammonia PET-MPI results, we categorized the territories of the RCA, LAD, and LCX as non-ischemic or ischemic. Ischemic territory was defined as a territory that consisted of one or more segments of ischemia.
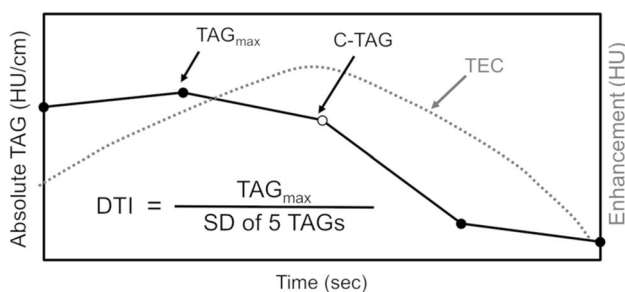

Fig. 2 Calculation of the dynamic TAG index (DTI). The DTI was defined as the ratio of the TAG_{max} to the standard deviation of five TAGs, which are at five phases around the peak enhancement. *C-TAG* the TAG at the boost scan, *TEC* time enhancement curve

The CT radiation dose of the dynamic CCTA

We recorded the machine-generated volume CT dose index (mGy) and the dose-length product (DLP) for each dynamic CCTA scan. We also estimated the effective radiation dose to the chest using the following equation [31]:

$$\text{Effective radiation dose} = \text{DLP} \times 0.026(\text{mSv}).$$

Statistical analyses

All statistical analyses were performed using JMP vs. 13 software (SAS, Cary, NC, USA). Continuous variables are expressed as the mean ± SD, and categorical variables are expressed as frequencies and percentages. The DTI and C-TAG values for coronary territories with and without ischemia were compared using the Wilcoxon rank-sum test. We performed a receiver operating characteristic (ROC) curve analysis to determine the optimal cutoffs of the DTI and C-TAG for identifying ischemia as defined based on PET-MPI results [32]. Optimal cutoffs were determined by values with Youden J statistics. The incremental values of the DTI and the C-TAG to standard CCTA-derived diameter stenosis at ≥ 50% for the presence of ischemia were determined by comparing the respective area under the ROC curve (AUC) using the method of DeLong [33]. Probability values < 0.05 were accepted as significant.

Results

The results obtained with ^{13}N-ammonia PET-MPI and standard CCTA

The ^{13}N-ammonia PET-MPI detected 27 ischemic territories (RCA, $n = 8$; LAD, $n = 10$; LCX, $n = 9$) in 22 of the 48 patients, and thus in the remaining 26 patients, no ischemic territory was observed. Of 22 patients with ischemic territory, two patients have prior myocardial infarction. We therefore used 27 ischemic and 117 normal territories as analytic targets.

We excluded five coronary arteries with severe stenosis or occlusion, seven arteries with motion artifacts, and six arteries with insufficient enhancement from the analysis because the DTI could not be measured. The DTI and the C-TAG were analyzed for a final total of 89 normal coronary arteries (RCA, $n = 36$; LAD, $n = 22$; LCX, $n = 31$) and 37 coronary arteries with ≥ 50% stenosis (RCA, $n = 9$; LAD, $n = 19$; LCX, $n = 9$). 88% of coronary artery could be evaluated by the DTI and C-TAG.

According to the ^{13}N-ammonia PET-MPI results, the 37 territories with $\geq 50\%$ stenosis consisted of 11 ischemic territories (30%) and 26 normal territories (70%). The 89 territories without stenosis consisted of 10 ischemic territories (11%) and 79 normal territories (89%).

The detection of ischemia by the DTI

The DTI was significantly higher for ischemia (8.8 ± 3.9) compared to non-ischemia (4.6 ± 2.0, $p < 0.01$). There was no significant difference in the C-TAG between the ischemia and non-ischemia groups (24.9 ± 9.0 vs. 20.9 ± 17.8 HU/cm, respectively; $p = 0.19$) (Fig. 3).

The ROC analysis revealed the DTI of 5.60 as the optimal cutoff to detect ischemia, with an AUC of 0.87, 85.7% sensitivity, and 76.2% specificity. For the C-TAG, 20.4 was the optimal cutoff point for detecting ischemia, with an AUC of 0.62, 76.2% sensitivity, and 57.1% specificity (Fig. 4). Representative cases are shown in Figs. 5 and 6.
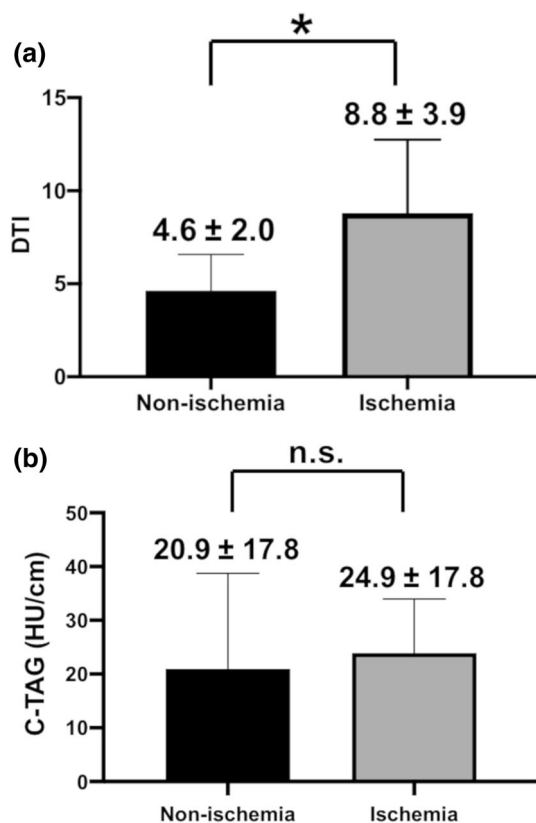
Fig. 3 Comparison of the DTI (**a**) and the C-TAG (**b**) between ischemic and non-ischemic coronary territories. The DTI was significantly higher for ischemia than for non-ischemia. *$p < 0.01$, n.s. not significant
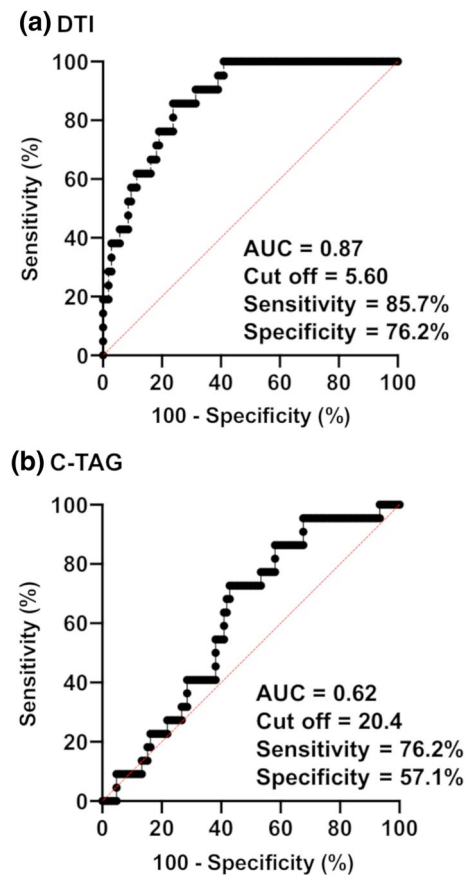
Fig. 4 ROC curves for the DTI and the C-TAG for ischemia. **a** DTI. **b** C-TAG. The AUC of the DTI was higher than that of the C-TAG

The incremental diagnostic values of the DTI and the C-TAG for the presence of ischemia

The results of the ROC analyses regarding the incremental diagnostic values of the DTI and the C-TAG to CCTA-derived diameter stenosis alone for the presence of ischemia (as defined by PET-MPI) are illustrated in Fig. 7. The AUC was 0.89 (95%CI 0.78–0.99) for DTI + CCTA, 0.73 (95%CI 0.57–0.90) for C-TAG + CCTA, and 0.64 (95%CI 0.50–0.78) for CCTA alone. The addition of the DTI to CCTA significantly increased the AUC for the presence of ischemia ($p = 0.0097$). The addition of the C-TAG to CCTA did not significantly increase the AUC ($p = 0.3622$).

The radiation dose of dynamic CCTA and ^{13}N-ammonia PET-MPI

The mean effective radiation dose was 8.6 ± 1.8 mSv for the dynamic CCTA. The mean effective radiation dose was 3.3 ± 0.1 mSv for ^{13}N-ammonia PET-MPI.
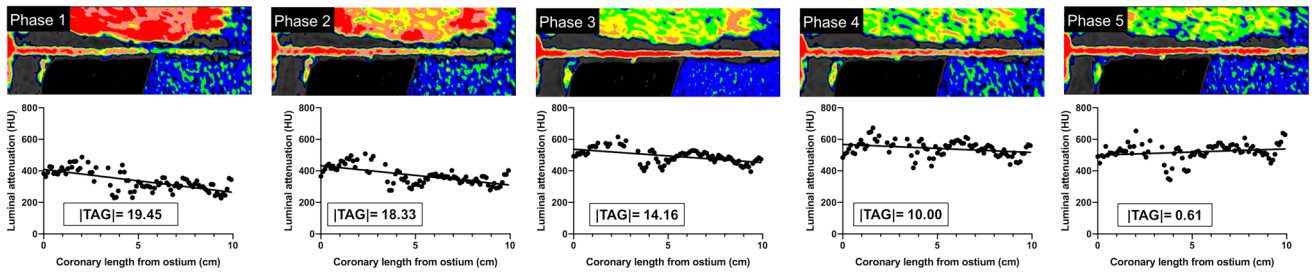
Fig. 5 Straightened curved multiplanar reconstruction (MPR) images of the RCA and the TAGs at five different phases for a 46-year-old man with non-ischemia on PET-MPI. Moderate stenosis was observed in the patient's mid-RCA on CCTA. According to luminal attenuation (HU), the lumen of the coronary artery was delineated by a six-color scale. Warm colors represent high CT values, and cold colors represent low CT values. The change in the five TAGs was large, resulting in the DTI of 2.85
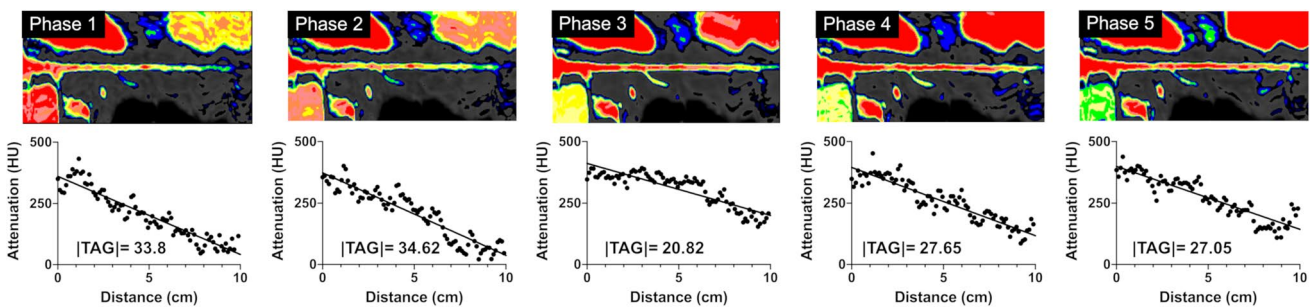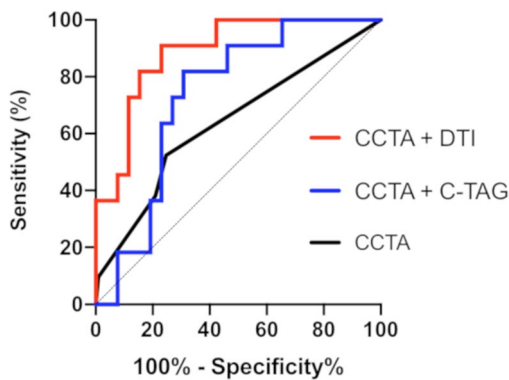

Fig. 6 Straightened curved MPR images of the LCX and the TAGs at five different phases for an 80-year-old man with ischemia on PET-MPI. The patient had no significant coronary stenosis on CCTA. The color scale of the coronary artery is the same as in Fig. 5. The change in the five TAGs was small, resulting in the DTI of 6.88

Test	AUC	95% CI	P-value
CCTA	0.64	0.50 - 0.78	-
CCTA + DTI	0.89	0.78 - 0.99	0.0097
CCTA + C-TAG	0.73	0.57 - 0.90	0.3622

Fig. 7 The diagnostic value of coronary CTA alone vs. coronary CTA with the DTI or the C-TAG for the presence of ischemia. The addition of the DTI to CCTA significantly increased the AUC for the presence of ischemia ($p = 0.0097$). The addition of the C-TAG to CCTA did not significantly increase the AUC ($p = 0.36$)

Discussion

We assessed the diagnostic potential of the DTI and TAG for the presence of ischemia as defined by ^{13}N-ammonia PET-MPI. Our analyses revealed that the DTI for ischemia was significantly higher than that for non-ischemia. However, there was no significant difference in the TAG between the ischemia and non-ischemia.

Several research groups reported that the use of TAG provided no additional diagnostic value for the assessment of the hemodynamic consequences of coronary stenosis [17, 18, 34, 35]. The major reasons for this are that TAG may be affected not only by ischemia but also by other factors such as the scanning method (volume or helical scanning) [36], the scan timing after the CM injection, and the injection methods (test bolus or bolus tracking). In our study, TAG was calculated using whole-heart volume scanning and the test-bolus method that was recommended for TAG analyses in a previous report [19]. However, our present findings are also in line with those of earlier studies [17, 18, 34, 35]. We observed that the use of TAG

provided no additional diagnostic value for the detection of ischemia.

We thus propose the novel DTI index, which incorporates the following two important points — which were reported by Funama et al. [19] — in TAG analyses. First, TAG depends on the scan timing after the injection of the CM. The scan time to the peak contrast enhancement of coronary arteries is not appropriate for obtaining the optimal TAG value. We adjusted this timing by applying the maximum absolute TAG from the five phases around the peak enhancement of the coronary artery into the numerator of the DTI equation. Second, the variation in the TAGs without significant stenosis was larger than the variation in the TAGs with significant stenosis at the scan timing after the CM injection. We compensated for this by plugging the standard deviation (SD) of five TAGs into the denominator of the DTI equation. This SD reflects the contrast enhancement delay. We speculate that these two points make it possible that compared to a TAG, the DTI is more likely to reflect directly coronary flow. At the time of measuring TAG, the attenuation measurement along the center line of the coronary artery lumen is performed while avoiding the calcification of the vessels' wall. Therefore, the DTI is less affected by coronary calcification.

Our present findings demonstrate that the DTI provided incremental diagnostic value over CCTA alone for the presence of ischemia as defined by PET-MPI. Several studies have shown that an anatomic assessment by CCTA using > 50% diameter stenosis does not correlate well with the functional assessment [2–4]. Similarly, based on the PET-MPI results in the present study, 27 cases with > 50% stenosis as shown by CCTA were diagnosed as normal. Of these, 19 (73%) cases were correctly diagnosed as normal by the DTI. Conversely, ten cases with < 50% stenosis by CCTA were diagnosed as ischemic. Of these, eight cases (80%) were correctly diagnosed as ischemic by the DTI. These results suggest that the use of the DTI combined with CCTA is more helpful in the functional assessment of coronary arteries. Hybrid analyses of the DTI and coronary stenosis derived from dynamic CCTA could have diagnostic ability that is comparable to that of stress/rest PET-MPI. Our method also reduces the burden on the patient because only the rest scan is taken.

Ideally, the anatomic and functional significance of coronary artery stenosis should be determined by a single noninvasive imaging examination. A hybrid analysis of DTI and CCTA results derived from dynamic CCTA can be performed for functional and anatomic assessments with a single contrast injection and a CT examination without additional cost or special software. The mean time for post-processing analysis of the DTI was 20 min. It is possible to analyze and obtain results immediately after CCTA scan. Moreover, this imaging technique can also visualize the coronary flow for dynamic color-coding [37].

There are some advantages of CT approach respect to ^{13}N-ammonia PET-MPI in terms of availability. First, the cost of CCTA is about one-third that of PET. Second, there can be more than ten CCTA examinations per day. On the other hand, there is a limit to the amount of ammonia produced by the cyclotron, and only three examinations per day are possible. Third, the CT examination time is approximately 30 min, which is shorter than the PET examination time of approximately 70 min. The features of DTI technique were summarized as follows: (1) direct coronary flow quantification, (2) data can be obtained from routine clinical workup, and (3) it can contribute as additional functional test over standard CCTA interpretation.

This study has several limitations. First, this study is a retrospective single-center study, the patient cohort is relatively small. Our findings thus require confirmation in larger multicenter studies. Second, coronary arteries with a cross-sectional area > 2.0 mm^2 appear to be necessary for a DTI analysis, because the vessel centerline and contouring cannot be accurately extracted in smaller arteries. The application of the DTI in smaller vessels may be a limitation. Third, the calculation of DTI requires 320-slice CT scanner that enables a single volume scan for the whole heart, and 64- or 128-slice CT scanners is not suitable. Moreover, the utility of the DTI must also be validated using more current acquisition and reconstruction protocols, such as the model-based iterative reconstruction or deep learning-based reconstruction which can reduce image noise [38, 39]. These reconstruction methods may be useful for obese patients with high image noise. Fourth, sufficient contrast enhancement and less motion artifacts of coronary arteries at continuous five data must be achieved to determine the DTI. In this study, the rate of exclusion from the analysis of coronary segments due to these effects was 9% of the whole dynamic images.

PET analysis was limited to visual evaluation using SDS and no quantitative evaluation was performed. Myocardial blood flow and myocardial flow reserve are affected by age, lifestyle-related diseases, renal function, and microvascular disease. In this study, ischemic diagnosis by SDS was used as a standard to make one-to-one correspondence between coronary arteries and their perfusion regions.

Conclusion

We proposed the DTI as a novel coronary flow index for use with dynamic CCTA. The DTI value for ischemia was significantly higher than that for non-ischemia, and its use added value to coronary CTA for the detection of myocardial ischemia. Hybrid analyses of the DTI and CCTA results derived from dynamic CCTA can be performed for

functional and anatomic imaging with a single contrast injection and a CT examination.

Compliance with ethical standards

Conflict of interest The authors declare that they have no conflict of interest.

References

1. Budoff MJ, Dowe D, Jollis JG, Gitter M, Sutherland J, Halamert E, Scherer M, Bellinger R, Martin A, Benton R, Delago A, Min JK (2008) Diagnostic performance of 64-multidetector row coronary computed tomographic angiography for evaluation of coronary artery stenosis in individuals without known coronary artery disease: results from the prospective multicenter ACCURACY (Assessment by Coronary Computed Tomographic Angiography of Individuals Undergoing Invasive Coronary Angiography) trial. J Am Coll Cardiol 52(21):1724–1732

2. Kern MJ, Lerman A, Bech JW, De Bruyne B, Eeckhout E, Fearon WF, Higano ST, Lim MJ, Meuwissen M, Piek JJ, Pijls NH, Siebes M, Spaan JA, American Heart Association Committee on Diagnostic and Interventional Cardiac Catheterization, Council on Clinical Cardiology (2006) Physiological assessment of coronary artery disease in the cardiac catheterization laboratory: a scientific statement from the American Heart Association Committee on Diagnostic and Interventional Cardiac Catheterization Council on Clinical Cardiology. Circulation 114(12):1321–1341

3. Tobis J, Azarbal B, Slavin L (2007) Assessment of intermediate severity coronary lesions in the catheterization laboratory. J Am Coll Cardiol 49(8):839–848

4. Wong DT, Ko BS, Cameron JD, Leong DP, Leung MC, Malaiapan Y, Nerlekar N, Crossett M, Troupis J, Meredith IT, Seneviratne SK (2014) Comparison of diagnostic accuracy of combined assessment using adenosine stress computed tomography perfusion + computed tomography angiography with transluminal attenuation gradient + computed tomography angiography against invasive fractional flow reserve. J Am Coll Cardiol 63(18):1904–1912

5. Wong DT, Ko BS, Cameron JD, Nerlekar N, Leung MC, Malaiapan Y, Crossett M, Leong DP, Worthley SG, Troupis J, Meredith IT, Seneviratne SK (2013) Transluminal attenuation gradient in coronary computed tomography angiography is a novel noninvasive approach to the identification of functionally significant coronary artery stenosis: a comparison with fractional flow reserve. J Am Coll Cardiol 61(12):1271–1279

6. Steigner ML, Mitsouras D, Whitmore AG, Otero HJ, Wang C, Buckley O, Levit NA, Hussain AZ, Cai T, Mather RT, Smedby O, DiCarli MF, Rybicki FJ (2010) Iodinated contrast opacification gradients in normal coronary arteries imaged with prospectively ECG-gated single heart beat 320-detector row computed tomography. Circ Cardiovasc Imaging 3(2):179–186

7. Zheng M, Wei M, Wen D, Zhao H, Liu Y, Li J, Li J (2015) Transluminal attenuation gradient in coronary computed tomography angiography for determining stenosis severity of calcified coronary artery: a primary study with dual-source CT. Eur Radiol 25(5):1219–1228

8. Takx RA, Blomberg BA, El Aidi H, Habets J, de Jong PA, Nagel E, Hoffmann U, Leiner T (2015) Diagnostic accuracy of stress myocardial perfusion imaging compared to invasive coronary angiography with fractional flow reserve meta-analysis. Circ Cardiovasc Imaging 8(1):e002666

9. Rochitte CE, George RT, Chen MY, Arbab-Zadeh A, Dewey M, Miller JM, Niinuma H, Yoshioka K, Kitagawa K, Nakamori S, Laham R, Vavere AL, Cerci RJ, Mehra VC, Nomura C, Kofoed KF, Jinzaki M, Kuribayashi S, de Roos A, Laule M, Tan SY, Hoe J, Paul N, Rybicki FJ, Brinker JA, Arai AE, Cox C, Clouse ME, Di Carli MF, Lima JAC (2014) Computed tomography angiography and perfusion to assess coronary artery stenosis causing perfusion defects by single photon emission computed tomography: the CORE320 study. Eur Heart J 35(17):1120–1130

10. Tanabe Y, Kido T, Uetani T, Kurata A, Kono T, Ogimoto A, Miyagawa M, Soma T, Murase K, Iwaki H, Mochizuki T (2016) Differentiation of myocardial ischemia and infarction assessed by dynamic computed tomography perfusion imaging and comparison with cardiac magnetic resonance and single-photon emission computed tomography. Eur Radiol 26(11):3790–3801

11. Norgaard BL, Leipsic J, Gaur S, Seneviratne S, Ko BS, Ito H, Jensen JM, Mauri L, De Bruyne B, Bezerra H, Osawa K, Marwan M, Naber C, Erglis A, Park SJ, Christiansen EH, Kaltoft A, Lassen JF, Botker HE, Achenbach S (2014) Diagnostic performance of noninvasive fractional flow reserve derived from coronary computed tomography angiography in suspected coronary artery disease: the NXT trial (Analysis of Coronary Blood Flow Using CT Angiography: Next Steps). J Am Coll Cardiol 63(12):1145–1155

12. Nakazato R, Park HB, Berman DS, Gransar H, Koo BK, Erglis A, Lin FY, Dunning AM, Budoff MJ, Malpeso J, Leipsic J, Min JK (2013) Noninvasive fractional flow reserve derived from computed tomography angiography for coronary lesions of intermediate stenosis severity results from the DeFACTO Study. Circ Cardiovasc Imaging 6(6):881–889

13. Miyajima K, Motoyama S, Sarai M, Kawai H, Nagahara Y, Matsumoto R, Fujiwara W, Muramatsu T, Takahashi H, Naruse H, Ishii J, Kondo T, Narula J, Izawa H, Ozaki Y (2020) On-site assessment of computed tomography-derived fractional flow reserve in comparison with myocardial perfusion imaging and invasive fractional flow reserve. Heart Vessels 35(10):1331–1340. https://doi.org/10.1007/s00380-00020-01606-z

14. Nagata K, Tanaka R, Takagi H, Fusazaki T, Morino Y, Yoshioka K (2018) Improved diagnostic performance of transluminal attenuation gradient in combination with morphological evaluation of coronary artery stenosis using 320-row computed tomography. Jpn J Radiol 36(1):51–58

15. Choi JH, Kim EK, Kim SM, Song YB, Hahn JY, Choi SH, Gwon HC, Lee SH, Choe YH, Oh JK (2014) Noninvasive evaluation of coronary collateral arterial flow by coronary computed tomographic angiography. Circ Cardiovasc Imaging 7(3):482–490

16. Choi JH, Min JK, Labounty TM, Lin FY, Mendoza DD, Shin DH, Ariaratnam NS, Koduru S, Granada JF, Gerber TC, Oh JK, Gwon HC, Choe YH (2011) Intracoronary transluminal attenuation gradient in coronary CT angiography for determining coronary artery stenosis. JACC Cardiovasc Imaging 4(11):1149–1157

17. Wang R, Renker M, Schoepf UJ, Wichmann JL, Fuller SR, Rier JD, Bayer RR, Steinberg DH, De Cecco CN, Baumann S (2015) Diagnostic value of quantitative stenosis predictors with coronary CT angiography compared to invasive fractional flow reserve. Eur J Radiol 84(8):1509–1515

18. Stuijfzand WJ, Danad I, Raijmakers PG, Marcu CB, Heymans MW, van Kuijk CC, van Rossum AC, Nieman K, Min JK, Leipsic J, van Royen N, Knaapen P (2014) Additional value of transluminal attenuation gradient in CT angiography to predict hemodynamic significance of coronary artery stenosis. JACC Cardiovasc Imaging 7(4):374–386

19. Funama Y, Utsunomiya D, Oda S, Shimonobo T, Nakaura T, Mukunoki T, Kidoh M, Yuki H, Yamashita Y (2016) Transluminal attenuation-gradient coronary CT angiography on a 320-MDCT volume scanner: Effect of scan timing, coronary artery stenosis,

and cardiac output using a contrast medium flow phantom. Phys Med 32(11):1415–1421

20. Tamaki N, Yonekura Y, Konishi J, Senda M, Yamashita K, Koide H, Saji H, Hashimoto T, Fudo T, Kambara H, Kawai C (1988) Value and limitation of stress thallium-201 single photon emission computed tomography: comparison with nitrogen-13 ammonia positron tomography. J Nucl Med 29(7):1181–1188

21. Husmann L, Wiegand M, Valenta I, Gaemperli O, Schepis T, Siegrist PT, Namdar M, Wyss CA, Alkadhi H, Kaufmann PA (2008) Diagnostic accuracy of myocardial perfusion imaging with single photon emission computed tomography and positron emission tomography: a comparison with coronary angiography. Int J Cardiovasc Imaging 24(5):511–551

22. Di Carli MF, Hachamovitch R (2007) New technology for non-invasive evaluation of coronary artery disease. Circulation 115(11):1464–1480

23. Fathala A, Aboulkheir M, Shoukri MM, Alsergani H (2019) Diagnostic accuracy of (13)N-ammonia myocardial perfusion imaging with PET-CT in the detection of coronary artery disease. Cardiovasc Diagn Ther 9(1):35–42

24. Jaarsma C, Leiner T, Bekkers SC, Crijns HJ, Wildberger JE, Nagel E, Nelemans PJ, Schalla S (2012) Diagnostic performance of noninvasive myocardial perfusion imaging using single-photon emission computed tomography, cardiac magnetic resonance, and positron emission tomography imaging for the detection of obstructive coronary artery disease: a meta-analysis. J Am Coll Cardiol 59(19):1719–1728

25. Driessen RS, Raijmakers PG, Stuijfzand WJ, Knaapen P (2017) Myocardial perfusion imaging with PET. Int J Cardiovasc Imaging 33(7):1021–1031

26. Bateman TM, Dilsizian V, Beanlands RS, DePuey EG, Heller GV, Wolinsky DA (2016) American Society of Nuclear Cardiology and Society of Nuclear Medicine and molecular imaging joint position statement on the clinical indications for myocardial perfusion PET. J Nucl Cardiol 23(5):1227–1231

27. Shirasaka T, Nagao M, Yamasaki Y, Kojima T, Kondo M, Shimomiya Y, Kamitani T, Honda H (2019) Feasible scan timing for 320-row coronary CT angiography generated by the time to peak in the ascending aorta. Clin Imaging 54:153–158

28. Austen WG, Edwards JE, Frye RL, Gensini GG, Gott VL, Griffith LS, McGoon DC, Murphy ML, Roe BB (1975) A reporting system on patients evaluated for coronary artery disease. Report of the Ad Hoc Committee for Grading of Coronary Artery Disease, Council on Cardiovascular Surgery American Heart Association. Circulation 51(4 Suppl):5–40

29. Ko BS, Wong DT, Norgaard BL, Leong DP, Cameron JD, Gaur S, Marwan M, Achenbach S, Kuribayashi S, Kimura T, Meredith IT, Seneviratne SK (2016) Diagnostic performance of transluminal attenuation gradient and noninvasive fractional flow reserve derived from 320-detector row CT angiography to diagnose hemodynamically significant coronary stenosis: an NXT substudy. Radiology 279(1):75–83

30. Kato E, Fujimoto S, Takamura K, Kawaguchi Y, Aoshima C, Hiki M, Kumamaru KK, Daida H (2018) Clinical significance of transluminal attenuation gradient in 320-row area detector coronary CT angiography. Heart Vessels 33(5):462–469

31. Trattner S, Halliburton S, Thompson CM, Xu Y, Chelliah A, Jambawalikar SR, Peng B, Peters MR, Jacobs JE, Ghesani M, Jang JJ, Al-Khalidi H, Einstein AJ (2018) Cardiac-Specific conversion factors to estimate radiation effective dose from dose-length product in computed tomography. JACC Cardiovasc Imaging 11(1):64–74

32. Metz CE (2008) ROC analysis in medical imaging: a tutorial review of the literature. Radiol Phys Technol 1(1):2–12

33. DeLong ER, DeLong DM, Clarke-Pearson DL (1988) Comparing the areas under two or more correlated receiver operating characteristic curves: a nonparametric approach. Biometrics 44(3):837–845

34. Bom MJ, Driessen RS, Stuijfzand WJ, Raijmakers PG, Van Kuijk CC, Lammertsma AA, van Rossum AC, van Royen N, Knuuti J, Mäki M, Nieman K, Min JK, Leipsic JA, Danad I, Knaapen P (2019) Diagnostic value of transluminal attenuation gradient for the presence of ischemia as defined by fractional flow reserve and quantitative positron emission tomography. JACC Cardiovasc Imaging 12(2):323–333

35. Park EA, Lee W, Park SJ, Kim YK, Hwang HY (2016) Influence of coronary artery diameter on intracoronary transluminal attenuation gradient during CT angiography. JACC Cardiovasc Imaging 9(9):1074–1083

36. Xu L, Sun Z, Fan Z (2015) Noninvasive physiologic assessment of coronary stenoses using cardiac CT. Biomed Res Int 2015:435737

37. Nagao M, Yamasaki Y, Kamitani T, Kawanami S, Sagiyama K, Yamanouchi T, Shimomiya Y, Matoba T, Mukai Y, Odashiro K, Baba S, Maruoka Y, Kitamura Y, Nishie A, Honda H (2016) Quantification of coronary flow using dynamic angiography with 320-detector row CT and motion coherence image processing: Detection of ischemia for intermediate coronary stenosis. Eur J Radiol 85(5):996–1003

38. Maeda E, Tomizawa N, Kanno S, Yasaka K, Kubo T, Ino K, Torigoe R, Ohtomo K (2017) The feasibility of Forward-projected model-based Iterative Reconstruction SoluTion (FIRST) for coronary 320-row computed tomography angiography: a pilot study. J Cardiovasc Comput Tomogr 11(1):40–45

39. Tatsugami F, Higaki T, Nakamura Y, Yu Z, Zhou J, Lu Y, Fujioka C, Kitagawa T, Kihara Y, Iida M, Awai K (2019) Deep learning-based image restoration algorithm for coronary CT angiography. Eur Radiol 29(10):5322–5329